A MODEL FOR DYNAMIC ANALYSIS OF A 5PK BELT TRANSMISSION IN DRY OR WET CONDITIONS

KRZYSZTOF KUBAS[1]
University of Bielsko-Biała

Summary

A belt transmission model with dry or partially wet belt models used for dynamic analysis has been presented in this paper. A two-dimensional discrete model was created, consisting of rigid elements connected with each other by means of longitudinal and torsional spring-damping elements (SDEs). The belt-pulley contact phenomena were described with the use of a model with appropriate stiffness and damping between the contacting surfaces and a simplified Threlfall friction model was used to describe the friction phenomenon. Motion of the transmission is triggered under the influence of torque loads applied on the pulleys. Calculations results are presented of reaction, contact and friction forces acting on dry and partially wet belt. Finally, an example of using the model to analyse the dynamics of a wet automotive belt transmission system driving the alternator and coolant pump has been presented.

Keywords: belt transmissions, dynamics analysis, friction, poly-V belt, wet belt

1. Introduction

Deliberations on the phenomena occurring in belt transmission systems date back to the 18th century and they were initiated by Leonard Euler [6]. The first main paper of research works confirming the existence of the phenomenon of micro-displacements in belt transmissions were presented, is the study by Reynolds [13] dated 1847. The major research works carried out over the centuries, with the most important works being specified in more detail, have been presented by Fawcett in the widely quoted publication [7]. It is worth adding here that works on chain transmissions have also been discussed in that publication.

Nowadays, belt transmissions are becoming more and more common. The good insulation against vibrations transmitted by the driving pulley or the relatively low mass of such systems are in certain situations the factors that are decisive for the superiority of such transmissions over other systems. Undoubtedly, this growing popularity stems from

[1] University of Bielsko-Biała, Faculty of Mechanical Engineering and Computer Science, Department of Mechanics, ul. Willowa 2, 43-309 Bielsko-Biała, e-mail: kkubas@ath.bielsko.pl

their increasing reliability, which in turn is an effect of the application of better solutions, especially the belts. What is meant here is both the use of more and more reliable materials and development in the belt engineering (belt shaping, type and layout of the load-carrying layer, etc.).

The theoretical coefficient of efficiency of a belt transmission should exceed 90%. Alas, many transmissions of this kind work with an efficiency being far below this level. This may be due to a variety of reasons, such as incorrect design or assembly of the transmission system (including incorrect belt tension or pulley misalignment) or improper maintenance or operation of the system. The most common faults of belt transmission operators include insufficiently frequent inspection of the transmission belt during its operation. The inspection should include not only the checking of belt tension or damage but also searching for possible contaminations. On the other hand, even such aspects might be investigated with the use of an appropriate computer model of the transmission system, e.g. for examining the impact of transmission defects on its efficiency.

It should remember that the transmission may be contaminated with both solids (such as stones, sand, dust) and liquids (eg oil and water). As a result of the presence of contaminants in the transmission – both the solid and liquid – there may occur different types of damage belt, among which can be mentioned: the excessive wear, chipping (breakage in the lower part), the formation of spongy or sticky structure on its surface, twisting the belt in the groove, excessive wear of the ribs (in the case of ribbed belts), or even breaking [17]. Contaminated belt transmission not only provides faster wear of its components, often leading to damage of the belt but also decreases the transmission efficiency and increases energy losses. The consequences of poorly designed and supported belt transmissions can be found in works [15, 17]. In present article has been presented model with both clean (dry) and contaminated (with water) conditions included.

The necessity of introducing steadily improved solutions is connected with a series of tests of successive prototypes, carried out on appropriate test stands. This often results in a significant growth in costs. A way to reduce the costs may be the construction of a "virtual prototype", i.e. a computer model that would enable preliminary selection of optimum belt characteristics.

From the point of view of the assumptions made in the model presented herein, the studies where discrete belt models have been presented ([8, 11, 12]) seem to be particularly important.

The study of belt transmissions under conditions conductive to the presence of water or ice layer between the belt and the pulley and the effect on the value of the coefficient of friction were involved in such the Authors of [1, 14]. The conclusion after carrying out the literature presenting studies of contaminated belt transmissions is that such works are few.

The normal forces acting on the pulley, necessary for determining the said friction forces, can be established with the use of a spring-damping model [2, 4, 12] (also referred to as a "penalty contact model"). Such a model was used in this study, too.

Moreover, a system of rigid elements connected with each other by means of spring-damping elements was adopted to represent the belt in the belt transmission model shown in this study. In transmissions of this type, the belt is subjected in most cases to significant strains caused by bending, e.g. on curved surfaces of pulleys and tensioner idlers, if any; therefore, an assumption was made that a relatively large number of elements would have to be used to discretize the belt. Obviously, this affects the computation speed and, in consequence, the time of carrying out the analyses. Undoubtedly, there are many good points of the discretization of a transmission belt. They include e.g. the possibility of identifying changes in the friction forces along the circumference of a pulley or distribution of the axial forces along the entire belt length.

Presented paper is the continuation of earlier works. In paper [10] was created model of belt transmission with friction model including creep. In article [9] it was presented simpler model assuming friction model similar to proposed model by Threlfall [16]. In these articles also proved a good agreement of these models with other presented by another Authors [2]. Both of them are two-dimensional discrete models.

In present article will be shown a modified model from paper [9]. In this model also introduced the possibility of changing friction coefficient on the circumference of the belt. It allowed to include impurities in part of belt. The impurity taken into the consideration will be a water.

2. Mathematical model

It was assumed that transmission consists of n_p pulleys. The belt was assumed to consist of n_{el} elements. Each of the elements was connected with the neighbouring ones by means of spring-damping elements (hereafter referred to as SDE) with appropriate longitudinal or torsional rigidity and damping values (Fig. 1a).

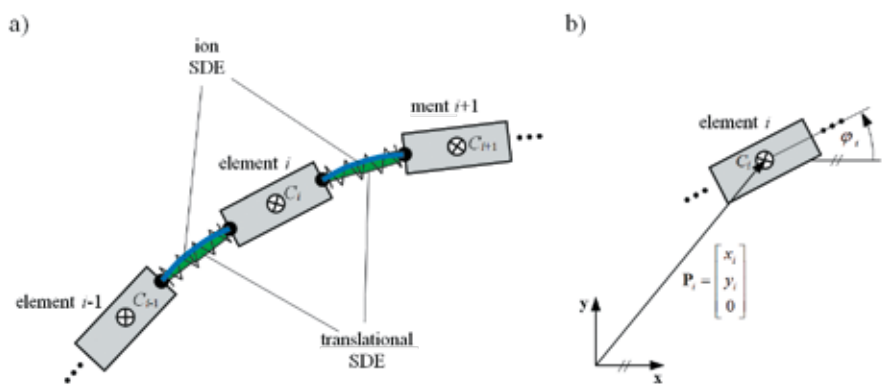

Fig. 1. The belt model assumed: a) longitudinal and torsional SDEs; b) generalized coordinates defining the location and orientation of element *i* of the belt

As mentioned above, a two-dimensional model was to represent the belt transmission system. For every element i (where $i = 1...n_{el}$), three generalized coordinates were adopted, i.e. displacements x_i and y_i of its centre of mass in relation to axes $\mathbf{x}$ and $\mathbf{y}$ of the global coordinate system and angle φ_i of rotation of the element in relation to its centre of mass (Fig. 1b). The value of coordinate z_i was zero. The position of the centre of mass of belt element i was defined by means of vector $\mathbf{P}_i$, as shown in Fig. 1b.

Moreover, an assumption was made that the transmission included np pulleys situated within plane $\mathbf{xy}$ and rotating around an axis parallel to axis $\mathbf{z}$ by angle Θ_j (where $j = 1...n_p$). This means that the vector of the generalized coordinates could be presented in the following form:

$$\mathbf{q}^T = \left[\mathbf{q}_{el}^T \,\vdots\, \mathbf{q}_p^T\right] = \left[x_1 \;\; y_1 \;\; \varphi_1 \;\; \dots \;\; x_i \;\; y_i \;\; \varphi_i \;\; \dots \;\; x_{n_{el}} \;\; y_{n_{el}} \;\; \varphi_{n_{el}} \,\vdots\, \theta_1 \;\; \dots \;\; \theta_j \;\; \dots \;\; \theta_{n_p}\right], \tag{1}$$

where: $\mathbf{q}_{el}$ – vector of the generalized coordinates of all the belt elements;

$\mathbf{q}_p$ – vector of the generalized coordinates of all the pulleys.

According to the assumptions made, the total number of the generalized coordinates was $3n_{el} + n_p$.

For the contact between belt elements and pulleys to be taken into account in the transmission model, the vector notation of forces was used. A schematic diagram of the assumed system of forces acting on element i of the belt when the element is in contact with pulley j has been shown in Fig. 2.

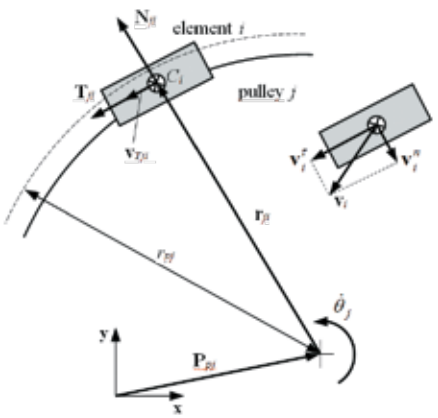

Fig. 2. The assumed system of belt element *i* velocity components and forces applied to this belt element by pulley *j*

It was assumed that the component forces, i.e. the normal forces $\mathbf{N}_{ji}$ and friction $\mathbf{T}_{ji}$, were applied to the centre of mass of each of the belt elements being in contact with the pulley. Such an assumption is acceptable if the belt thickness is disregarded (thanks to which

e.g. the nature of stresses in the belt cross-section is not analysed and the friction force may be reduced to centre C_i) and a sufficiently large number of elements is adopted to discretize the belt, which translates into sufficiently small lengths of the belt elements. It is also worth mentioning here that the assumptions made are consistent with the current trends in the designing of transmission belts, according to which the belt height is minimized to reduce the transverse deformations and thus to increase the transverse stiffness of the belt [5].

As it can be seen in Fig. 2, vector $\mathbf{r}_{ji}$ was drawn from the centre of pulley j to the centre of mass of belt element i. At the instant when the belt element comes into contact with the pulley but the value of normal force $\mathbf{N}_{ji}$ is still zero, the length of this vector is equal to an arbitrarily selected value r_{pj}. Hence, for a non-zero normal force, the following inequality holds: $r_{ji} < r_{pj}$. The position of the pulley centre in the global coordinate system was defined by vector $\mathbf{P}_{pj}$.

The value of normal force was determined in a form similar to that presented in study [3], where the non-linear relationship between deformation and force was proven:

$$N_{ji}\left(p_{ji}, \dot{p}_{ji}\right) = c_1 \cdot p_{ji}^2 + c_2 \cdot p_{ji} + \delta\left(p_{ji}\right) \cdot b \cdot \dot{p}_{ji}, \tag{2}$$

where: c_1, c_2 – stiffness coefficients of the belt-pulley contact;
b – damping coefficient of the belt-pulley contact;
p_{max} – assumed arbitrary value of reached "full damping".

A graphical representation of the function $\delta(p_{ji})$ has been presented in Fig. 3.

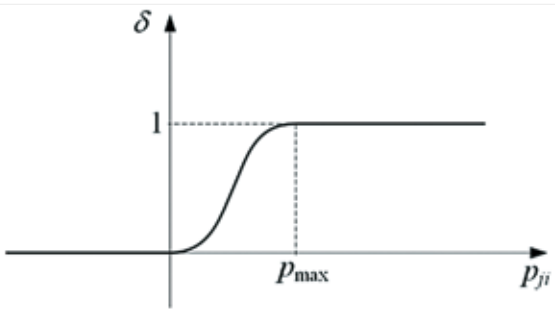

Fig. 3. Graphical representation of the function $\delta(p_{ji})$

Thanks to the application of formula (2), the force component resulting from damping at the belt and pulley interface depends not only on the penetration velocity $\dot{p}_{ji}$ but also on the penetration depth p_{ji}. Taking into account the coefficient $\delta(p_{ji})$ helped to avoid sticking of belt elements with the pulleys, especially, when the relative velocity is large in the phase of starting contact. It should be simultaneously stressed that these relationships are universally used in models of contact. A similar model has been used e.g. in the MSC. ADAMS software [19].

Fig. 4 shows the assumed simplified form of the coefficient of friction as adopted by Threlfall [16]. As it can be seen in the graph, the value Δv is an arbitrarily chosen level of the velocity v, from which the coefficient of friction is assumed to take the value of μk appropriate for kinetic friction.

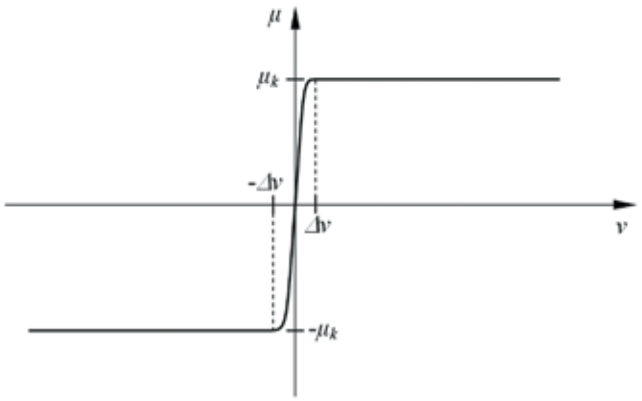

Fig. 4. Simplified form of the characteristic curve of the coefficient of friction [16]

The above characteristic curve is usually adopted with assuming identical values for the static and kinematic friction ($\mu_s = \mu_k$). As it has been shown in publication [3], the values of these coefficients may actually be close to each other; therefore, a decision was made to use a simplified model presented in Fig. 4 in this work as well. The Coulomb formula, used for determining the value of friction force $\mathbf{T}$, takes the following form in this case:

$$T = \mu(v) \cdot N. \tag{3}$$

Finally, the friction force was defined by the equation:

$$\mathbf{T}_{ji} = \boldsymbol{\mu}_{ji}(\mathbf{v}_{Tji}) \cdot N_{ji}, \tag{4}$$

where: $\boldsymbol{\mu}_{ji}(\mathbf{v}_{Tji}) = \mu_{ji}(v_{Tji})\hat{\mathbf{v}}_{Tji}$ – coefficient of friction of i-th element acting on j-th pulley in vector notation;

$\mathbf{v}_{Tji}$ – vector of relative velocity;

$\hat{\mathbf{v}}_{Tji}$ – versor whose direction and sense are consistent with those of vector $\mathbf{v}_{Tji}$.

Fig. 5 shows a schematic diagram of the adopted system of forces and moments applied to belt element i by the neighbouring belt elements.

The values of the reaction forces and torques in the longitudinal and torsional SDEs that connect element i – 1 with element i were described by equations known in the literature as the Kelvin-Voigt equations [18]:

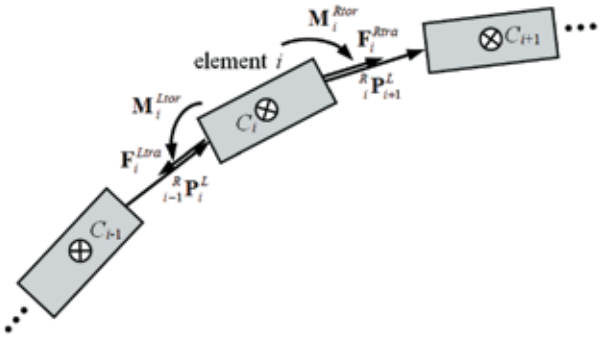

Fig. 5. System of forces and moments applied to belt element *i* by the neighbouring elements

$$F_i^{Ltra} = F_{i-1}^{Rtra} = c_{tra}\left(\Delta l_i^L\right)^{e_{tra}} + b_{tra}\Delta \dot{l}_i^L, \tag{5}$$

$$M_i^{Ltor} = M_{i-1}^{Rtor} = c_{tor}\left(\varphi_i - \varphi_{i-1}\right)^{e_{tor}} + b_{tor}\left(\dot{\varphi}_i - \dot{\varphi}_{i-1}\right), \tag{6}$$

where: F_i^{Ltra}, F_i^{Rtra} – values of the reaction forces in the left and right longitudinal SDE (that connect belt element i with element i – 1 and belt element i with element i + 1, respectively);

M_i^{Ltor}, M_i^{Rtor} – values of the torsional torques in the left and right torsional SDE, respectively;

c_{tra}, b_{tra} – stiffness and damping coefficient, respectively, of the longitudinal SDE of the belt;

c_{tor}, b_{tor} – stiffness and damping coefficient, respectively, of the torsional SDE of the belt;

e_{tra}, e_{tor} – exponential coefficients being measures of the longitudinal and torsional stiffness, respectively, of the SDE of the belt;

Δl_i^L – deformation of the longitudinal SDE of the belt;

$\Delta \dot{l}_i^L$ – rate of deformation of the longitudinal SDE of the belt.

The equations of motion were derived with the use of the Newton-Euler formalism. The equations of motion of belt element i take the form:

$$\begin{cases} m_i\ddot{x}_i = (\mathbf{F}_i^{Ltra} + \mathbf{F}_i^{Rtra} + \sum_{j=0}^{n_p-1}(\mathbf{N}_{ji} + \mathbf{T}_{ji}) + m_i\mathbf{g})\cdot\mathbf{X}^T, \\ m_i\ddot{y}_i = (\mathbf{F}_i^{Ltra} + \mathbf{F}_i^{Rtra} + \sum_{j=0}^{n_p-1}(\mathbf{N}_{ji} + \mathbf{T}_{ji}) + m_i\mathbf{g})\cdot\mathbf{Y}^T, \\ I_{z_i}\ddot{\varphi}_i = (\mathbf{M}_i^{Ltra} + \mathbf{M}_i^{Rtra} + \mathbf{M}_i^{Ltor} + \mathbf{M}_i^{Rtor})\cdot\mathbf{Z}^T, \end{cases} \tag{7}$$

where: $\hat{\mathbf{X}}^T = [1\,0\,0]$, $\hat{\mathbf{Y}}^T = [0\,1\,0]$, $\hat{\mathbf{Z}}^T = [0\,0\,1]$ – versors whose directions and senses are consistent with those of axes $\mathbf{x}$, $\mathbf{y}$, and $\mathbf{z}$ of the global coordinate system;

$$\mathbf{M}_i^{Ltra} = -\mathbf{l}'_i \times \mathbf{F}_i^{Ltra};$$

$$\mathbf{M}_i^{Rtra} = \mathbf{l}'_i \times \mathbf{F}_i^{Rtra};$$

$$\mathbf{l}'_i = \begin{bmatrix} \frac{l_i}{2}\cos\varphi_i \\ \frac{l_i}{2}\sin\varphi_i \\ 0 \end{bmatrix}$$ – vector defining the direction and half-length of belt element i (vector $\mathbf{l}'_{i-1}$ is determined likewise);

$\mathbf{g}$ – acceleration of gravity.

As it can be easily noticed, equations (7) can be simplified. So, appropriate components of the vectors specified in brackets should be substituted on the right side of the equality signs.

It was assumed that the pulleys would move under the impact of driving torques applied. The equation of motion of pulley j will have the form:

$$I_{z_j}\ddot{\theta}_j = M_{dj} - \sum_{i=0}^{n_d-1} \mathbf{M}_{Tji} \cdot \mathbf{Z}^T, \tag{8}$$

where: I_{z_j} – mass moment of inertia of pulley j;

M_{dj} – driving torque value;

$\mathbf{M}_{Tji} = \mathbf{r}_{ji} \times \mathbf{T}_{ji}$ – moment of the friction force resulting from the impact of belt element i on the pulley.

The differential equations of motion were solved with the use of the Runge-Kutta-Fehlberg method with variable-step integration. The calculation results were generated in the form of appropriate time histories with the use of the MATLAB environment.

3. Calculations results

Belt parameters based on publications [2, 3, 4] were taken into account. In the works described there, the Authors took on the task to determine the parameters of longitudinal and torsional stiffness of the belt and the parameters that were necessary for taking into account the phenomena related to the belt-pulley contact, i.e. the stiffness and damping in the model of this contact and the coefficients of friction. Following the information provided in publications [3, 4], the analysis was carried out for a multi-rib belt (also referred to as serpentine belt, multi-grooved belt, poly-V belt, etc.) model 5pk. Belts of this type are used in transmission systems that are heavily loaded and/or operate in the conditions of high rotational velocities.

In Fig. 6 presented assumed model of the belt transmission with adopted parameters. There were no tensioners in the transmission system under analysis and the driving and driven pulleys had identical radii equal to $r_{p1} = r_{p2} = r_p = 0.1$ m. The distance between pulley centres was $l_p = 0.29$ m. The belt model adopted for analyses consisted of 60 elements of identical length.

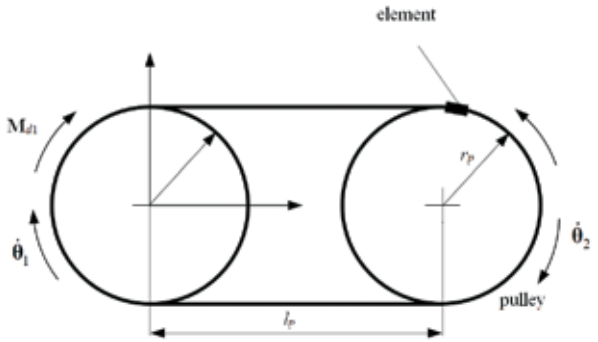

Fig. 6. The assumed model of the belt transmission system with dry belt

The belt was pre-tensioned to a belt force about 500 N. The parameters of the transmission system subjected to the analysis were adopted in accordance with the information found in publications [3, 4]:

$c_{tra} = 1.52 \cdot 10^5$ N/m, $b_{tra} = 20.5$ Ns/m, $c_{tor} = 0.026$ Nm/rad,
$b_{tor} = 0.05$ Nms/rad, $c_1 = 3.0256 \cdot 10^9$ N/m^2, $c_2 = 6.5 \cdot 10^5$ N/m,
$b = 300$ Ns/m, $p_{max} = 0.001$ m, $\Delta v = 10^{-5}$ m/s,
$\Delta_{max} = 10^{-4}$ m, $m_i = 0.096 \cdot l_i$ kg.

First, it has been assumed belt transmission model with dry belt. The values of the coefficients of dry friction were assumed to be identical for all length of the belt acting on both pulleys and they were adopted as $\mu_{ji} = 1$ (where $j = 1..n_p$, i = $1..n_{el}$) .

The global coordinate system was so established that its origin coincided with the centre of the driving pulley, axis $\mathbf{y}$ was directed oppositely to the gravitation force vector (i.e. upwards), and axis $\mathbf{x}$ was directed towards the centre of the driven pulley.

A force-type input in the form of a driving torque was adopted for the analysis. The driving torque $\mathbf{M}d_1$ on the driving pulley was represented by the torque vs. time curve shown in Fig. 7a (the direction and sense of this torque have been shown in Fig. 6). According to these assumptions, the driving torque was to grow within a time of 0.3 s to a level of 70 Nm and after this time, this torque value was to remain constant.

Moreover, the value of the resistance torque $\mathbf{M}d_2$ on the driven pulley was assumed to depend on the angular velocity of that pulley and the torque value of 70 Nm (i.e. equal to that of the driving torque on the driving pulley) was to be reached at a pulley velocity of

700 rpm. A curve representing this torque has been shown in Fig. 7b (the direction and sense of this torque have been shown in Fig. 6). As it can be seen in the graphs, the driving and resistance torques were realized in the form of a piecewise linear function and a linear function, respectively.

Such assumed values of applied forces should ensure relatively large belt load, with relatively not large working speed.

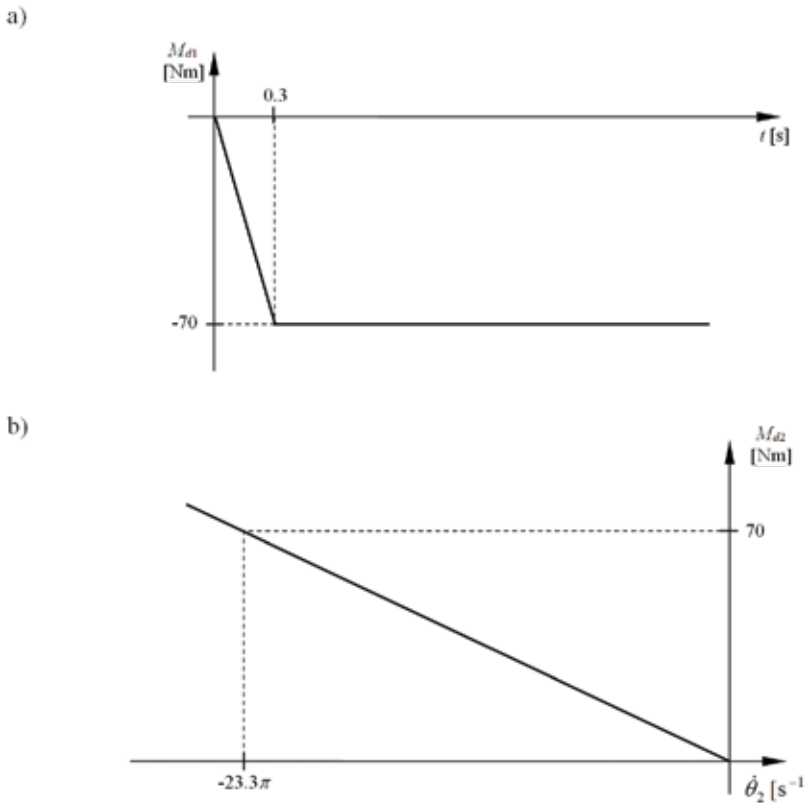

Fig. 7. Curves adopted to represent the input torques: a) driving torque on the driving pulley vs. time; b) resistance torque on the driven pulley vs. angular velocity

The resulting angular velocities of the driving and driven pulleys have been graphically presented in Fig. 8. When the test time exceeded 0.3 s, which corresponded to a growth in the torque value to about 70 Nm, the driving pulley angular velocity hasn't stabilized yet. After about 0.6 s has reached 68.5 rad/s and remained constant. This value is lower than could be expected, based on the input torques applied, because of energy dissipation in the SDEs in result of friction and damping in the belt-pulley contact model. Driven pulley angular velocity increased to about 68.0 rad/s. As can be therefore noticed, transmission slip is about 0.5 rad/s.

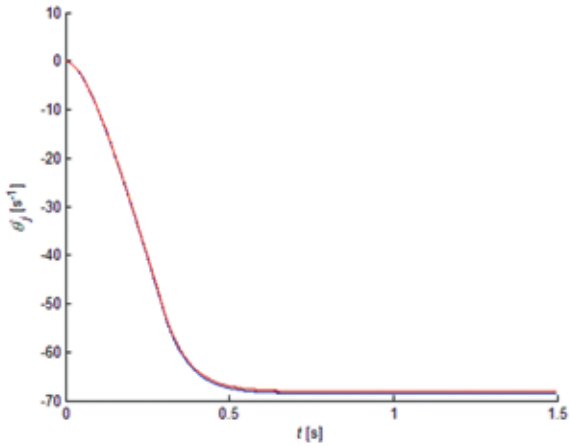

Fig. 8. Time histories of the angular velocities applied to the transmission pulleys, obtained from the model with dry belt: a) ——— driving pulley; b) ——— driven pulley

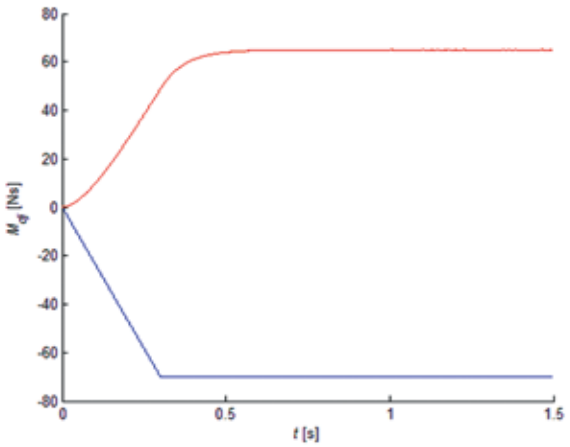

Fig.9. Time histories of torques applied to the transmission pulleys, obtained from the model with dry belt: a) ——— driving pulley; b) ——— driven pulley

Energy dissipation can be also seen on time histories of driving and resistance torques, shown in Fig. 9. Resistance torque of driven pulley reaches value about 65 Nm.

It was found reasonable to pay special attention to a specific belt element (marked in Fig. 6) taken together with the SDE being next to it to obtain the time histories of the forces applied to these parts by the pulleys and neighbouring belt elements. Fig. 10 shows the time history of the value of the reaction force in the selected longitudinal SDE.

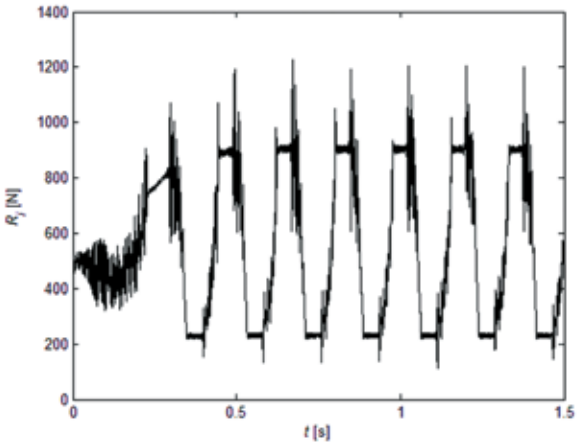

Fig. 10. Time history of the value of the reaction force in the selected longitudinal SDE, as obtained from the model with dry belt

As it can be seen in the graph, the force value changed stepwise. At the initial instant, when the transmission began its operation, a short period of system stabilization took place. Within the time range of up to 0.25 s, the SDE under analysis remained on lower side of the belt. The maximum value of force reached about 820 N. After this period, the force value rapidly changed to about 210 N and remained on this level in the time interval about 0.35 s to about 0.4 s. This was the time when the SDE was on the upper side of the belt. As can be seen from figure, these values are changing frequently during all simulation. The time intervals during which the force in the belt rapidly changed corresponded to the relatively short periods when the belt element under analysis was in contact with the transmission pulleys.

The next curves represent the values of the normal forces applied by the pulleys to the selected belt element (Fig. 11) and the values of the friction forces (Fig. 12) generated in result of the action of the normal forces.

According to the general knowledge of belt transmissions, available e.g. from publication [5], the normal force gradually decreases along the circumference of the driving pulley (observed in the direction from the driving side to the slack side of the belt) and gradually increases along the circumference of the driven pulley (observed in the direction from the slack side to the driving side of the belt). Such a relationship can be noticed in Fig. 12. In the graph, the analysed belt element first goes through the contact with the driven pulley (the first fragment representing the non-zero increasing values of the normal forces) and then it goes through the contact with the driving pulley (the second fragment representing the non-zero decreasing values of the normal forces).

It should be noticed, that courses shown in Fig.11 and 12 are very similar. Because it has been assumed friction coefficient equal unity (according to publication [3]), it must be

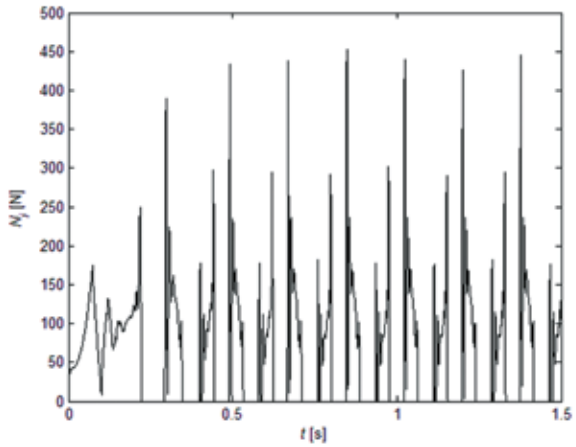

Fig. 11. Time history of the value of the normal forces applied by the pulleys to the selected belt element, as obtained from the model with dry belt

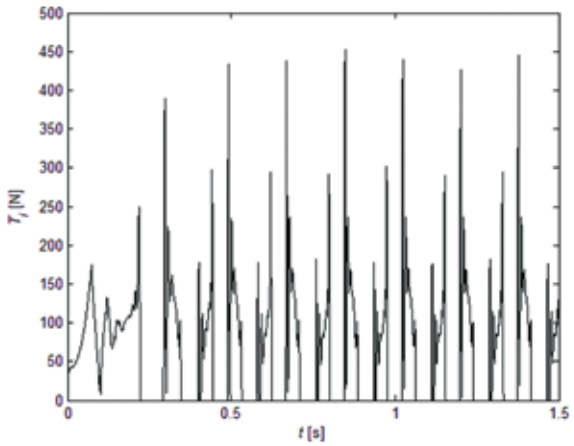

Fig. 12. Time history of the value of the friction forces at the contact between the pulleys and the selected belt element, as obtained from the model with dry belt

concluded that predominantly there are two cases of friction: maximum (fully developed) static friction or kinetic friction. As can be noticed from relative velocity course (Fig. 13), analysed belt element slips on the pulleys, but the slip velocity is relatively small.

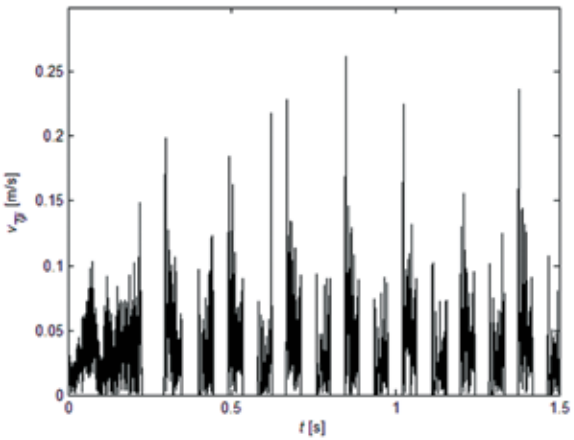

Fig. 13 Time history of the value of the element belt-pulleys relative velocity, as obtained from the model with dry belt

In next phase of analyses, it has been assumed that half of the belt will be wet. The model of the transmission is presented in Fig. 14. In the figure is also presented starting position of wet part of belt.

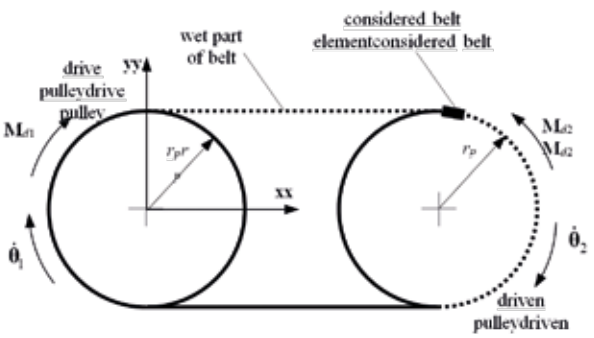

Fig. 14. The assumed model of transmission system with partially wet belt

In paper [17] Authors presented results of researches of belt transmission working in conditions with ice and water film on belt. They also presented time histories of changing friction coefficient. From this courses can be concluded, that in temperatures above 0°C, friction coefficient value is changing between 0 to 0.3. For present analyses it assumed $\mu_s = \mu_k$ = 0.2. It also assumed the same time histories of driving and resistance torques as applied in case of dry belt.

The time courses of the angular velocities of the pulleys of the model with partially wet belt have been presented in Fig. 15. It can be seen rapidly increasing angular velocity of driving pulley. At the end of simulation the velocity reaches value over 600 rad/s. The reason of increasing velocity is belt slip. Simultaneously, driven pulley rotates with angular velocity not exceeding 70 rad/s, so it is close to value obtained in case of dry belt. Additionally can be seen oscillating values of angular velocities of both pulleys. This is due to the successive changes of dry and wet parts of belt, which contact with the pulleys.

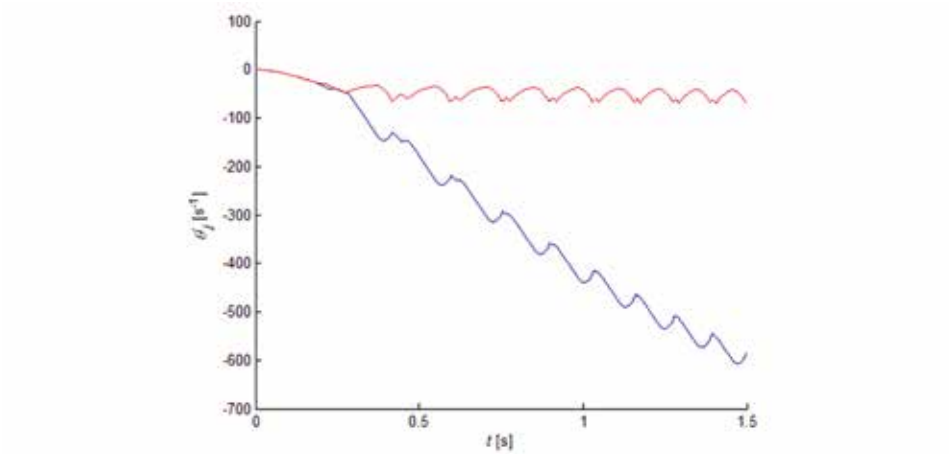

Fig. 15. Time histories of the angular velocities of the transmission pulleys, as obtained from the partially wet belt model: a) ——— driving pulley; b) ——— driven pulley

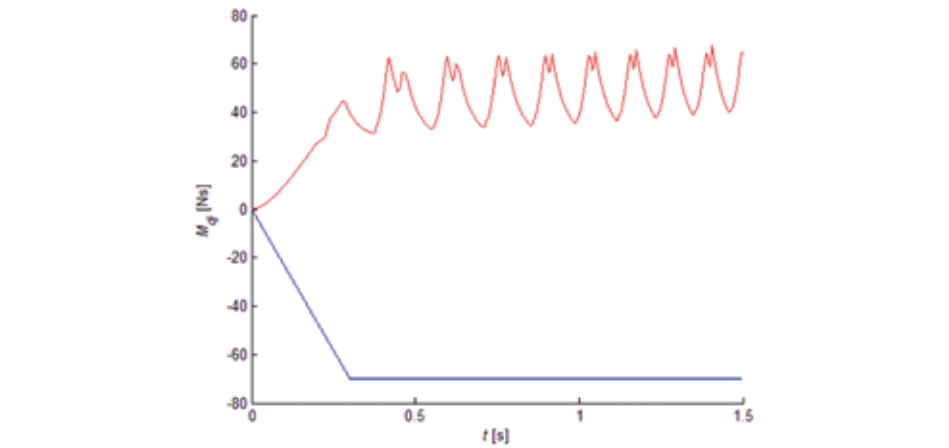

Fig. 16. Time histories of torques applied to the transmission pulleys, obtained from the model with partially wet belt: a) ——— driving pulley; b) ——— driven pulley

In Fig. 16 shown calculated time histories of driving and resistance torques acting on the pulleys. Comparing them with time histories in case of dry belt, can be seen that in this case resistance torque also not equals the driving torque. It is interesting, that the maximum values also reaches 65 Nm. In other hand there are seen oscillating values of resistance torque as result of oscillating values of its angular velocity.

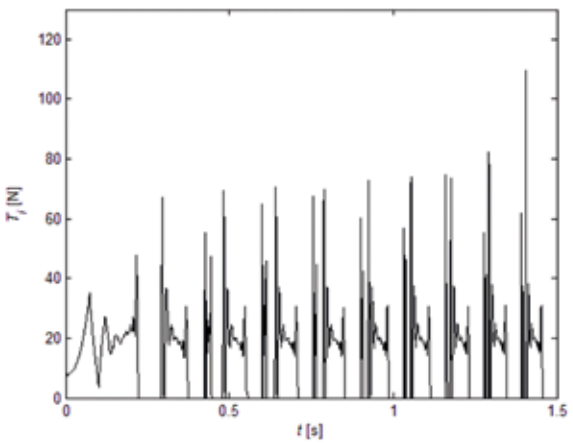

Fig.17. Time history of the value of the friction forces at the contact between the pulleys and the selected belt element, as obtained from the model with partially wet belt

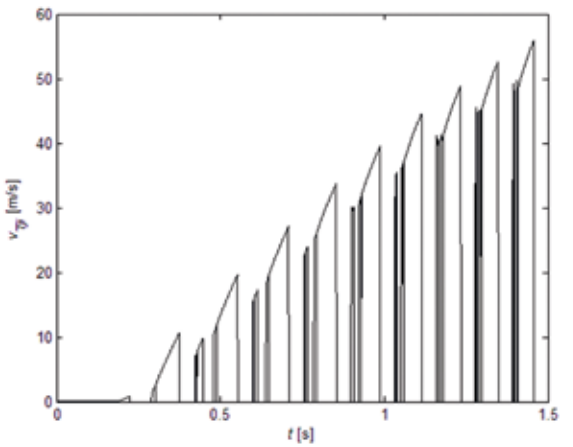

Fig. 18. Time history of the value of the element belt-pulley relative velocity, as obtained from the model with partially wet belt

It has been assumed that considered belt element will be located in the middle of wet part, (this element has been shown in Fig. 14). It can be seen from time history of friction force of this element (Fig. 17) that calculated values are much lower than shown

in Fig. 12. The values equal about 20% of values calculated in case of dry belt. So, they changed proportionally to assumed lower value of friction coefficient. Therefore, it is confirmed that in both cases belt transmission usually works with microslip or slip. It is also visible in time history of belt element-pulleys relative velocity (Fig. 18). Except starting phase, the velocity is greater then zero.

Additionally, can be seen much shorter time intervals of contact with driven pulley than with drive pulley. Because of acting centrifugal force and bending stiffness, with increasing belt velocity, the belt tends to deform. This deformation decreased contact area with the driven pulley. It is interesting that simultaneously it increased the area with the drive pulley.

4. Example belt transmission with a partially wet belt

An example of using the mathematical methods presented to analyse the dynamics of an automotive belt transmission system driving the alternator and coolant pump has been described below. This example has been also presented in earlier paper [9], but present model includes that 30% of belt is wet. The layout of the transmission system components taken into consideration has been illustrated in Fig. 19. As it can be seen, the transmission system included engine crankshaft, alternator, and coolant pump pulleys rotating clockwise and a tensioner idler rotating anticlockwise. The origin of the global coordinate system was adopted as coinciding with the centre of the alternator pulley. Additionally, it has been assumed the same driving torque, as shown in Fig. 7a, applied to engine crankshaft. It has also been assumed the same resistance torque (Fig. 7b) applied to the coolant pump pulley. These conditions correspond to situation, where coolant pump is defective (eg. has obliterated bearings). Rest of resistance torques are assumed as negligible.

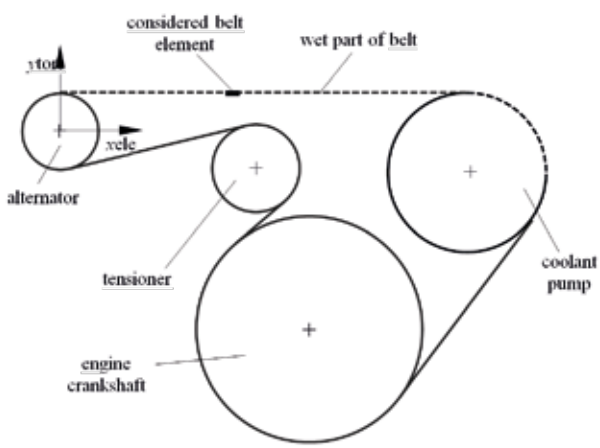

Fig. 19. Model of an automotive belt transmission system

The pulley radii were adopted as follows:

- engine crankshaft r_1 = 0.08 m;
- alternator r_2 = 0.027 m;
- coolant pump r_3 = 0.056 m;
- tensioner r_4 = 0.031 m.

The belt pretensioning force was adopted as 280 N. Number of elements were assumed as 150. The values of the parameters of stiffness and longitudinal and torsional damping of the SDEs and of the friction and contact between the belt and the pulleys were assumed as identical to those assumed in the preceding example. Due to the unavailability of data on the friction and contact between the belt and the tensioner idler, these data were assumed as having the same values as those of flat-belt pulleys.

The time histories of the angular velocities of the transmission components have been presented in Fig. 20. It can be seen in the graph that the values of angular velocity of the engine crankshaft, alternator, and coolant pump pulleys have been shown as negative while the tensioner idler has been shown to rotate with positive angular velocity values. This is because the positive sign was given to the anticlockwise direction of rotation and the clockwise direction of rotation was considered negative. It can be seen that just before 0.2 s velocities of the pulleys, except crankshaft, stop increasing. This is because the wet part of the belt started to slip on the crankshaft pulley. From this moment, crankshaft pulley angular velocity started rapidly increasing.

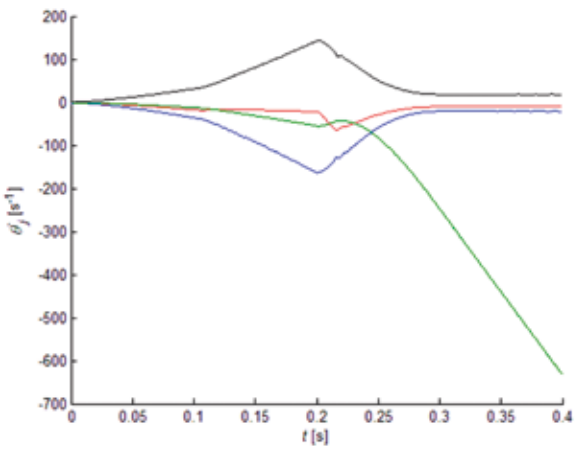

Fig. 20. Time histories of the angular velocities of the following transmission components, as obtained from the model: a) ——— engine crankshaft pulley; b) ——— alternator pulley; c) ——— coolant pump pulley; d) ——— tensioner idler

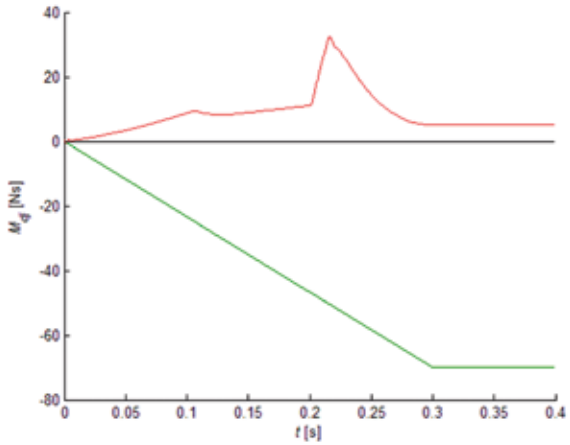

Fig. 21. Time histories of torques applied to the pulleys, as obtained from the model: a) ——— engine crankshaft pulley; b) ——— alternator pulley; c) ——— coolant pump pulley; d) ——— tensioner idler

Especially interesting is Fig. 21, where shown the time history of the values of the drive and resistance torques applied to the pulleys. In first phase (to about 0.22 s) the pulley of the coolant pump contact with wet part of belt. After that, this part goes due to the pulley of crankshaft, so the pulley of the coolant pump contact with dry part of belt. At this moment, the resistance torque increases rapidly to value about 30 Nm. Next, the pulley of the crankshaft started fully contact with wet part of belt, which cause increasing slip. Because of that, the velocity of the transmission (the belt) started decreasing.

The fact, that during simulation the analysed belt element (the position of this element at the initial position has been illustrated in Fig. 19) passes from the pulley of coolant pump to the pulley of the crankshaft is visible in time history of friction force (Fig. 22). Within the time range from 0.17 s to 0.2 s, considered belt element contacts with the pump pulley. In time from 0.26 s it starts contact with the pulley of crankshaft. Visible greater values of friction forces acting from the pump pulley are because of smaller radius than that of the crankshaft.

Fig. 23 shows time history of the values of the reaction force in the selected longitudinal SDE (element is located next to considered earlier rigid element). Significant increase of the force value at the time about 0.22 s is because of the fact, that the pump pulley only connects with dry part of belt (this increase can be also visible in Fig. 21). In this moment, the analysed SDE is located between the pump pulley and crankshaft pulley. The value of this force equals about 890 N. This value represents about 80% of value calculated from summarizing the driving and resistance torques.

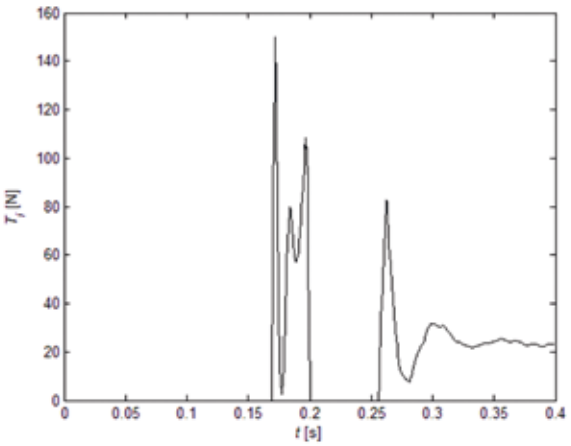

Fig. 22. Time history of the value of the friction forces applied by the pulleys to the selected belt element, as obtained from the model

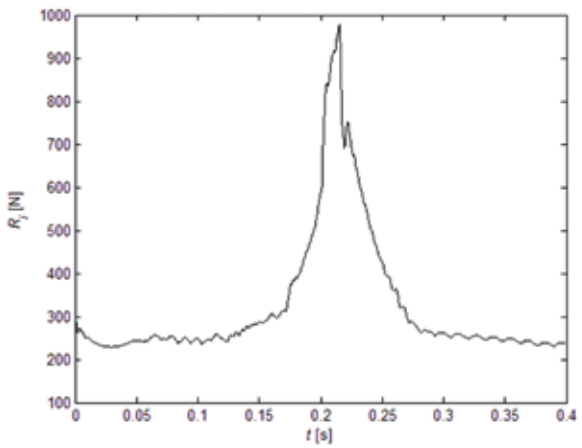

Fig. 23. Time history of the value of the reaction force in the selected longitudinal SDE, as obtained from the model

5. Conclusions

Proposed model is a continuation of earlier works presented in [9, 10], but first time is presented the model with impurities included.

Undoubtedly, created model should be verified using researches made on special research stand. Results of these researches would certainly complement the knowledge on discussed subject. It is especially important, because, as it was mentioned earlier, such type works aren't a lot. This studies will be the main subject of further author's investigations.

Additionally should be checked, which kind of friction is between clean and contaminated parts of the belt (of course, if it is partially contaminated). In this paper was assumed, that it isn't any transition area, in which there is mixed friction. The author is aware of that this simplification can lead the improper calculations results.

Maybe it should be necessary also to include the values of friction coefficients as functions of relative velocity in joint. It is planned to develop through researches the kinetic and dynamic characteristics of friction coefficient, which are determined in steady and variable velocities, respectively. It is also planned to investigate friction coefficients of other impurities, eg. oil.

References

[1] Bowden F.P.: Tabor D.: *The friction and lubrication of solids – Part II.* Oxford University Press, 1964.

[2] Čepon G., Boltežar M.: *Dynamics of a belt-drive system using a linear complementarity problem for the belt-pulley contact description.* Journal of Sound and Vibration, 319, 2009, pp.1019-1035.

[3] Čepon G., Manin L., Boltežar M.: *Experimental identification of the contact parameters between a V-ribbed belt and a pulley.* Mechanism and Machine Theory, 45, 2010, pp.1424-1433.

[4] Čepon G., Manin L., Boltežar M.: *Introduction of damping into the flexible multibody belt-drive model: A numerical and experimental investigation*. Journal of Sound and Vibration, 324, 2009, pp.283-296.

[5] Dahl P.R.: *A Solid Friction Model.* Report No. TOR-0158(3107-18)-1, Aerospace Corporation Report, 1968.

[6] Dudziak M.: *Przekładnie cięgnowe*. Wydawnictwo Naukowe PWN, Warszawa, 1997.

[7] Euler M.L.: *Remarques sur l'effect du frottement dans l'equilibre*. Mém. Acad. Sci., Berlin, 1762, pp. 265-278.

[8] Fawcett J.N.: *Chain and belt drives – a review*. Shock Vibrations Digest, 13(5), 1981, pp.5-12.

[9] Julio G., Plante J.-S.: *An experimentally-validated model of rubber-belt CVT mechanics.* Mechanism and Machine Theory, 46, 2011, pp.1037-1053.

[10] Kim D., Leamy M.J., Ferri A.A.: *Dynamic Modeling and Stability Analysis of Flat Belt Drives Using an Elastic/Perfectly Plastic Friction Law.* ASME Journal of Dynamic Systems, Measurement, and Control, 133, 2011, pp.1-10.

[11] Kragell'skij, I.V., Gitis N.V.: *Frikcionnye avtokolebanija.* Akademija Nauk SSSR, Nauka, Moskva, 1987.

[12] Leamy M.J., Wasfy T.M.: *Analysis of belt-drive mechanics using a creep-rate-dependent friction law*. Journal of Applied Mechanics, Trans. of ASME, 69, 2002, pp.763-771.

[13] Leamy M.J., Wasfy T.M.: *Dynamic finite element modeling of belt drives.* 18th Biennial Conference on Mechanical Vibration and Noise, ASME International 2001 DETC.

[14] Leamy M.J., Wasfy T.M.: *Transient and Steady-State Dynamic Finite Element Modeling of Belt-Drives*. ASME Journal of Dynamic Systems, Measurement, and Control, 124, 2002, pp. 575-581.

[15] Reynolds O.: *Creep theory of belt drive mechanics*. The Engineer, 38, 1847.

[16] Schindler T., Friedrich M., Ulbrich H.: *Computing time reduction possibilities in multibody dynamics, Multibody Dynamics: Computational Methods and Applications*. Dordrecht, Springer, 23, 2011, pp.239-259.

[17] Threfall D.C.: *The Inclusion of Coulomb Friction in Mechanisms Programs with Particular Reference to DRAM*. Mechanisms and Machine Theory, 13, 1978, pp.475-483.

[18] Voigt W.: *Ueber innere Reibung fester Körper, insbesondere der Metalle*. Annalon der Phisik, 283, pp.671-693, 1892.

[19] MSC.Adams documentation.